

# The Effect of Fluoride on the Size and Morphology of Apatite Crystals Grown from Physiologic Solutions

E. D. Eanes, A. W. Hailer

National Institute of Dental Research's Craniofacial and Skeletal Diseases Branch Research Associate Program, National Institute of Standards and Technology, Gaithersburg, Maryland 20899, USA

Received: 14 May 1997 / Accepted: 23 January 1998

**Abstract.** In adult human bone, fluoride uptake is accompanied by an increase in apatite crystal size. This increase, however, is not isotropic but is restricted primarily to growth in width and/or thickness, with no measurable change in length. In the present study, seeded growth experiments were conducted *in vitro* to determine whether this anisotropic effect is physicochemical in origin, i.e., a direct result of  $F^-$  selectively enhancing lateral crystal growth, or is an indirect consequence of  $F^-$ -induced alterations in cellular function and matrix development. The growth reactions were maintained at 37°C under physiologic-like solution conditions (1.33 mmol/liter  $Ca^{2+}$ , 1.0 mmol/liter total phosphate, 0 or 26 mmol/liter carbonate, 270 mmol/kg osmolality, pH 7.4) using constant-composition methods. When new accretions accumulated to three times the initial seed mass, the solids were collected and net crystal growth was assessed by X-ray diffraction line broadening analysis. The X-ray results revealed that the carbonate constituent in our physiologic-like solutions promoted the proliferation of new crystals at the expense of further growth of the seed apatite. Solution  $F^-$  concentrations of  $\sim 2 \mu\text{mol/liter}$  partially offset the repressive effect that carbonate had on primary crystal growth. Moreover,  $F^-$  stimulated seed crystal growth in the same anisotropic manner as had been observed for adult human bone apatite, a finding that suggests that the latter growth *in vivo* was the consequence, in part, of direct  $F^-$ -mineral interactions.

**Key words:** Apatite — Bone mineral — Calcification — Crystal texture — Fluoride.

Fluoride's strong affinity for the apatitic mineral phase in skeletal tissue is the major reason why nearly all ingested fluoride retained by the body is deposited in this tissue [1]. Fluoride concentrates for the most part in areas of bone tissue undergoing active mineralization [2, 3] where it easily

incorporates into hydroxide (OH) lattice sites during the nucleation and growth of the apatite crystals [4]. Because of the structural isomorphism between fluoridated and non-fluoridated apatites, this substitution occurs for the most part with little alteration in mineral composition. Of the two major lattice components, phosphate ( $PO_4$ ) is unaffected by fluoride, and calcium, at most, increases only slightly [3, 5–8]. Changes in most other chemical species such as  $Na^+$ ,  $Mg^{2+}$ , and carbonate also vary only slightly if at all [8–11].

In contrast to the chemical findings, improvements in the resolution of the X-ray diffraction profile of adult bone mineral suggest that substantial increases in apatite crystal size and/or lattice perfection accompany the uptake of fluoride [12–14]. Corresponding reductions in mineral surface area indicate further that the observed crystallinity changes could be accounted for by apatite crystal growth alone [15]. Such reductions could also explain the dramatic decreases in surface-adsorbed citrate anions, the only chemical species whose bone levels are significantly affected by fluoride uptake [10].

Of particular interest is the observation that these fluoride-associated changes do not affect all external crystal dimensions but instead, are restricted to increases in crystal width and/or thickness with no measurable change in length. This size anisotropy is most evident in bones from adult individuals who experienced prolonged exposure to high fluoride levels in their drinking water [13], although a similar effect has also been reported for cortical bone apatite of osteoporotic patients after long-term fluoride treatment [14]. It is presently unclear whether this anisotropic fluoride effect is physicochemical or metabolic in origin. However, its mechanistic elucidation could be of clinical relevance as the biomechanical quality of bone produced during fluoride treatment for osteoporosis may in some measure be determined by the change in the textural (i.e., size/shape) properties of the mineral component [16].

In the present study, the direct physicochemical effect that fluoride has on the texture of apatite crystals grown in seeded physiologic-like aqueous solutions was examined in an effort to better separate this effect from those brought about *in vivo* by fluoride-induced metabolic alterations in bone tissue.

## Materials and Methods

All seeded precipitation reactions were carried out in solutions initially 150 ml in volume, 1.33 mmol/liter in  $Ca^{2+}$ , 1.0 mmol/liter in total phosphate ( $tPO_4 = H_2PO_4^{1-} + HPO_4^{2-} + HPO_4^{3-}$ ), 0 or 26

Certain commercial materials and equipment are identified in this work for adequate definition of the experimental procedures. Such identification does not imply recommendation or endorsement by the National Institute of Standards and Technology or that the material and equipment identified is necessarily the best available for the purpose.

**Correspondence to:** E. D. Eanes, Building 224, Room A143, National Institute of Standards and Technology, Gaithersburg, MD 20899, USA

**Table 1.** Composition of starting and titrant solutions

Starting solution
1.33 mmol/liter $\text{Ca}(\text{NO}_3)_2$
1.00 mmol/liter $\text{KH}_2\text{PO}_4$
10.0 mmol/liter HEPES (pH 7.4)
143.0 mmol/liter $\text{KNO}_3$ or NaCl
(117.0 mmol/liter in carbonate experiments)
0–0.093 mmol/liter NaF (F/Ca = 0–0.07)
0 or 26 mmol/liter $\text{NaHCO}_3^a$
Calcium titrant
15.27 mmol/liter $\text{Ca}(\text{NO}_3)_2$
10.0 mmol/liter HEPES
Phosphate titrant
10.4 mmol/liter $\text{KH}_2\text{PO}_4$
(9.5 mmol/liter in carbonate experiments)
10.0 mmol/liter HEPES
260.8 mmol/liter $\text{KNO}_3$ or NaCl
(208.8 mmol/liter in carbonate experiments)
0–1.067 mmol/liter NaF (F/Ca = 0–0.07)
15.9 mmol/liter KOH
(14.5 mmol/liter in carbonate experiments)
0 or 52 mmol/liter $\text{NaHCO}_3^a$

<sup>a</sup> Added as a solid shortly before start of experiment

mmol/liter in carbonate ( $\text{CO}_3 = \text{HCO}_3^{1-} + \text{CO}_3^{2-}$ ), 0 or 0.8 mmol/liter in  $\text{Mg}^{2+}$ , and 0–0.093 mmol/liter in  $\text{F}^-$  (Table 1). The solutions also contained 10 mmol/liter HEPES (N-[2-hydroxyethyl]piperazine-N'-[2-ethanesulfonic acid]) and sufficient  $\text{KNO}_3$  or NaCl to bring the osmolality to 270 mmol/kg. Prior to seeding, the reaction solutions were adjusted to pH 7.4 with 0.01 mol/liter KOH and equilibrated between 36.9°C and 37.1°C for 1 hour in water-jacketed Nalgene Polypropylene vessels (Nalge Co., Rochester, NY) under presaturated  $\text{CO}_2$ -free  $\text{N}_2$  or, for the carbonate experiments, under 5%  $\text{CO}_2$ , 95%  $\text{N}_2$ . Reagent-grade chemicals and  $\text{CO}_2$ -free, distilled-deionized water were used in all solution preparations.

After 1 hour equilibration, each 150-ml reaction solution was seeded with 0.1 g dried apatite crystals (0.67 g/liter). The seed crystals were prepared by hydrolyzing freshly precipitated amorphous calcium phosphate for 1 hour at pH 7.4 and 37°C, as described in detail elsewhere [17]. X-ray diffraction and chemical analyses (described below) showed, respectively, that the apatite was comparable to bone mineral in crystal texture (i.e., less than 50 nm) and had a Ca/P molar ratio of 1.55, a value typical for pH 7.4 preparations [18]. Such finely textured apatite was used as a seed stock rather than well-crystallized material in order that growth could be easily assessed quantitatively by the X-ray line broadening methods described below. These crystals were also considered as better representing the texture of bioapatite crystals formed in actively mineralizing bone tissue [17, 19].

After being seeded, the precipitation reactions were sustained by the dual specific-ion electrode-controlled titration method of Ebrahimpour et al. [20] as adapted by Ishikawa et al. [17]. Initial solution supersaturation was maintained during the course of each reaction by simultaneously adding equal volumes of a  $\text{Ca}^{2+}$  titrant and a  $\text{tPO}_4$  titrant (Table 1) dispensed from separate motor-driven piston burets (Metrohm 655 Dosimat, Brinkmann Instruments, Westbury, NY) coupled in parallel electronically to a Metrohm 614 Impulsomat titrator. The latter, in turn, was controlled by a  $\text{Ca}^{2+}$ -ion electrode (Orion Research, Boston, MA) that maintained this ion at its preset concentration of 1.33 mmol/liter. The reactant concentrations (mmol/liter) in the titrant solutions were calculated as follows:

$$\begin{aligned} T_{\text{Ca}} &= 2(10 - x)C + 2(1.33) \\ T_{\text{tPO}_4} &= 2(6C) + 2(1.00) + B \\ T_{\text{OH}} &= 2(14 - 2x)C \end{aligned}$$

where (1.33) and (1.00) are the preset values (in mmol/liter) for the

**Table 2.** Total added  $\text{F}^-$  and solution  $\text{F}^-$  concentrations in seeded reaction suspensions when total titrant volume equaled  $3 \times$  the initial reaction volume

F/Ca <sup>a</sup>	Total F <sup>b</sup> ( $\mu\text{mol/liter}$ )	Solution F ( $\mu\text{mol/liter}$ )	% Total F in solution
0.005	30.3	<0.50	<1.65
0.010	60.6	$0.85 \pm 0.08$ (3) <sup>c</sup>	1.40
0.015	90.9	$1.14 \pm 0.16$ (3)	1.25
0.015 ( $\text{CO}_3$ ) <sup>d</sup>	90.9	$1.86 \pm 0.34$ (5)	2.05
0.070	424.2	$23.33 \pm 0.71$ (3)	5.50

<sup>a</sup> Molar F/Ca ratio of starting and titrant solutions

<sup>b</sup>  $\Sigma [(\text{Starting F}^- \text{ conc})(0.25) + (1/2 \text{ titrant F}^- \text{ conc.})(0.75)]$

<sup>c</sup> Mean  $\pm$  SD; values in ( ) = number of experiments

<sup>d</sup> Reaction carried out in 26 mmol/liter  $\text{NaHCO}_3$

solution  $\text{Ca}^{2+}$  and  $\text{tPO}_4$  concentrations, respectively, and C is the mmol/liter of precipitated apatite [ $\text{Ca}_{10-x}(\text{HPO}_4)_x(\text{PO}_4)_{6-x}(\text{OH})_{2-x}$ ]. The value of C was set at 0.7 mmol/liter, the molar equivalent of 0.67 g/liter of apatite used for seeding as based on the formula  $\text{Ca}_9\text{H}(\text{PO}_4)_6(\text{OH})$ . By setting C at this value, the solid/solution ratio of new solids formed during the course of the precipitation approximated the initial seed value. The B term in the  $T_{\text{tPO}_4}$  equation is an empirically determined adjustment to the  $\text{tPO}_4$  titrant concentration to compensate for slight deviations in solid Ca/ $\text{PO}_4$  ratios from 1.5. Also, for this reason, it was found that the reaction pH could be better controlled at 7.40 by reducing somewhat (<5%)  $T_{\text{OH}}$  in the  $\text{tPO}_4$  titrant solution and independently dispensing the remainder as a 0.01 mmol/liter KOH solution from a glass-electrode-controlled pH stat (Metrohm 702 SM Titrino). The HEPES buffer was used to minimize transient pH fluctuations with this arrangement [17].

In the fluoride experiments, independent control of solution  $\text{F}^-$  concentrations during seeded growth was not attempted. Instead, NaF was added to the starting and  $\text{tPO}_4$  titrant solutions at concentrations equal to 0, 0.005, 0.01, 0.015, or 0.07 times the starting and titrant  $\text{Ca}^{2+}$  concentrations, respectively (Table 1), i.e., starting solution  $\text{F}^-$  concentrations were 0, 6.67, 13.33, 20.0, or 93.3  $\mu\text{mol/liter}$  and the corresponding titrant concentrations were 11.5 times these values. Although overall F/Ca ratios were kept constant in this way, corresponding solution F/Ca ratios were reduced considerably from their initial values due to preferential  $\text{F}^-$  uptake by the precipitating solids (Table 2). In experiments containing  $\text{Mg}^{2+}$  and/or carbonate, the  $\text{Mg}^{2+}$  was added to the  $\text{Ca}^{2+}$  titrant and the carbonate was added to  $\text{PO}_4$  titrant at twice their respective initial solution concentrations (Table 1).

The ion activity products (IAP) of the starting solutions with respect to dicalcium phosphate dihydrate (DCPD), octacalcium phosphate (OCP), hydroxyapatite (OHAp), fluorapatite (FAP), and calcium fluoride ( $\text{CaF}_2$ ) were calculated using the procedure of McDowell et al. [21] and compared with the corresponding solubility products for these phases [21–24]. All starting solutions were determined to be supersaturated with respect to OHAp and OCP but undersaturated with respect to DCPD. Fluoride-containing starting solutions were supersaturated with respect to FAP but undersaturated with respect to  $\text{CaF}_2$ .

The status of the solution parameters was monitored at frequent intervals during the course of each experiment by collecting 2 ml aliquots of the reaction slurry, filtering the aliquots through 0.22  $\mu\text{m}$  Millex-GS filters (Millipore Corp., Bedford, MA), and analyzing the filtrates for  $\text{Ca}^{2+}$ ,  $\text{tPO}_4$ ,  $\text{F}^-$ , and  $\text{Mg}^{2+}$ .  $\text{Ca}^{2+}$  and  $\text{Mg}^{2+}$  were determined by atomic absorption spectrophotometry (Model 603, Perkin Elmer, Norwalk, CT),  $\text{tPO}_4$  by the spectrophotometric method of Murphy and Riley [25], and  $\text{F}^-$  potentiometrically with a specific ion electrode (Model 96-09 Combination F electrode, Orion Research). The solution  $\text{Ca}^{2+}$  and  $\text{tPO}_4$  concentrations stayed within 0.05 mmol/liter above or below their preset values. After an initial 14% drop, which occurred within the first 15 minutes,  $\text{Mg}^{2+}$  concentrations stabilized at 0.69 mmol/liter  $\pm$  0.02 mmol/liter (where the number following the symbol  $\pm$  is the stan-

dard deviation, SD). Solution  $F^-$  changes are described in the results.

When the total volume of titrants added during the precipitation reaction reached 450 ml (150 ml in the  $Mg^{2+}$  experiments), the slurry was vacuum filtered through 0.45  $\mu m$  nitrocellulose membrane filters (Schleicher and Schuell BA85, Keene, NH), and the retentate was washed with ice-cold ammoniated water and lyophilized. The lyophilized solids were analyzed chemically for  $Ca^{2+}$ ,  $Mg^{2+}$ ,  $tPO_4$ , and  $F^-$ . X-ray diffraction (XRD) patterns of the solids were recorded with a graphite-monochromatized Rigaku diffractometer (Rigaku, Danvers, MA) tuned to  $CuK\alpha$  radiation (wavelength 0.154 nm) generated at 35 kV and 20 mA. Because of extensive broadening of the apatitic profile of the seed crystals, only the 002 and 310 peaks were sufficiently resolved for quantitative measurement. Fortunately, these two peaks are associated with two mutually perpendicular crystalline dimensions, the length (002 peak) and width/thickness (310 peak). The 002 ( $24.5^\circ 2\theta$ – $27^\circ 2\theta$ , where  $2\theta$  signifies the angle between the incident and diffracted beams) and 310 ( $37.5^\circ 2\theta$ – $41.5^\circ 2\theta$ ) peaks of each sample were recorded a minimum of five times each at a scanning speed of  $0.125^\circ/\text{minute}$  (10 seconds time constant) with the intensity values numerically digitized at  $0.01^\circ$  intervals using special software developed by B. Dickens (National Institute of Standards and Technology, Gaithersburg, MD). The angular width of each 002 diffraction peak was measured at one half the height of maximum intensity above background and averaged. Standard deviations of the averaged values of these half-width (HW) measurements were less than  $0.015^\circ 2\theta$ . Since the 310 peak was partially overlapped by the weaker (20%) 212 apatite peak, the composite profile was averaged, then graphically matched to the sum of two Lorentzian functions, each representing one of the two overlapping diffraction peaks, using a nonlinear, curve-fitting software program (Peakfit 3.0, Jandel Scientific Software, San Rafael, CA). The HW value for the 310 peak was then obtained from the corresponding fitted Lorentzian function. For solids harvested from the  $F^-$  and carbonate experiments, the angular position of the Lorentzian function for the 310 peak was observed to be consistently higher than the seed value of  $39.70^\circ 2\theta$ . Although the shifts were slight ( $\leq 0.11^\circ 2\theta$ ), the lack of precise superpositioning of the scattered X-rays from the new accretions and from the original seed crystals had the effect of broadening the measured HW values. To correct for this peak shift broadening, the Peakfit analysis was modified to graphically subtract the Lorentzian function representing the seed contribution from the measured 310 peak profile. In carrying out this subtraction, values obtained from unreacted seed material were used for the position and HW parameters of the subtracted function. The intensity of this function was set at 0.25 the value of the observed 310 peak. The corrected HW values were then obtained from the Lorentzian function of the reduced 310 peak. Similar corrections were not required for the 002 peak. Since HW values correlate inversely with crystal size and lattice perfection [26], the reciprocals of the HW values ( $1/HW$ ) for the 002 and 310 peaks were used to relate the X-ray data more directly to these parameters along the length and width/thickness of the crystals, respectively. The composite "width/thickness" term is used to designate the crystal direction associated with the 310 peak as this latter direction is oblique to the lateral growth faces of apatite.

## Results

Under the physiologic-like solution conditions employed in this study, the addition of the apatite seeds initiated accretion reactions whose rates were dependent in varying degrees on the presence of fluoride, magnesium, and/or carbonate ions. As shown from the total volume of added titrants versus time curves in Figure 1, fluoride accelerated the addition of titrants to the reaction solution. This acceleration was dose-dependent in that the time it took new accretions to accumulate to three times the initial seed mass progressively decreased with increased fluoride concentration (Fig. 2). Physiologic carbonate concentrations showed

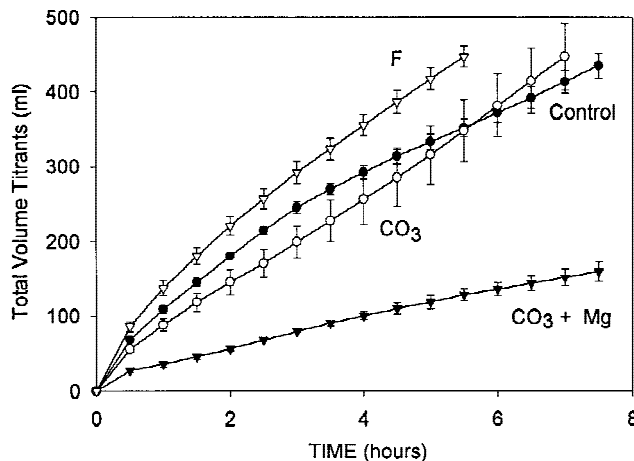


Fig. 1. Effects of fluoride,  $F/Ca = 0.015$  ( $\nabla$ ), carbonate, 26 mmol/liter ( $\circ$ ), and carbonate + magnesium, 0.8 mmol/liter ( $\blacktriangledown$ ) ions on the rate of addition of titrants in accretion reactions seeded with apatite crystals and maintained at 1.33 mmol/liter  $Ca^{2+}$  and 1.0 mmol/liter  $tPO_4$  (control,  $\bullet$ ). Values shown are means of triplicate reactions with SD shown as error bars.

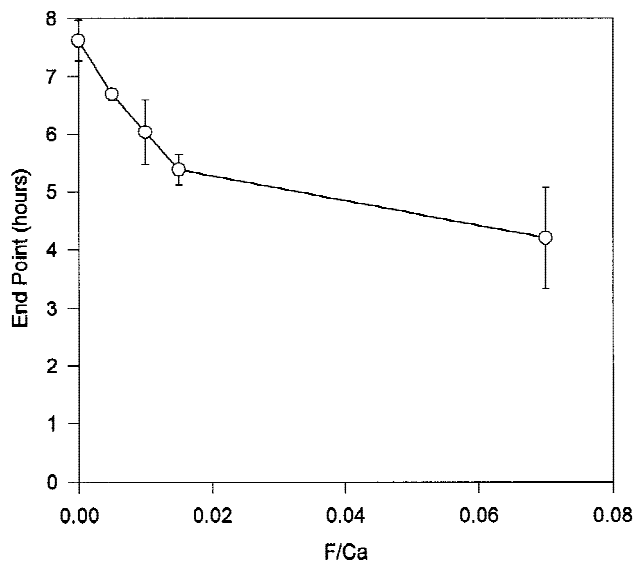
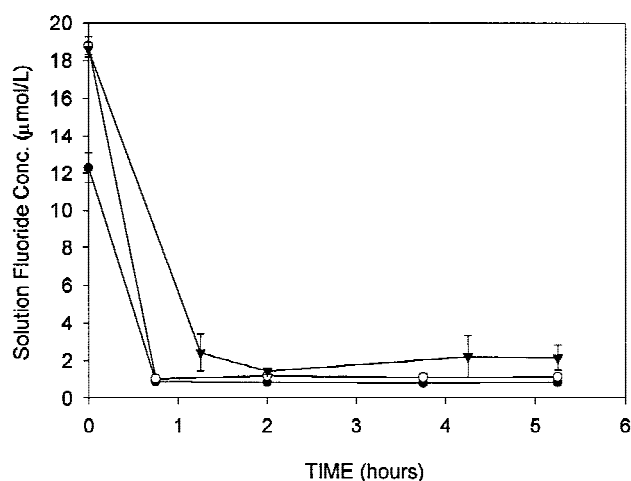


Fig. 2. Effect of overall  $F/Ca$  molar ratio on the time it took to reach the point in carbonate-free reactions at which new accretions equaled  $3\times$  initial seed mass. Error bars indicate SD of triplicate reactions (except  $n = 2$  for  $F/Ca = 0.005$ ).

a somewhat more complex behavior, initially slowing the reaction then accelerating it so that the time it took to reach the endpoint was essentially unchanged (Fig. 1). Adding  $F^-$  ( $F/Ca$  molar ratio = 0.015) to the carbonate medium, however, had the same accelerating effect on accretion as in carbonate-free solutions, with the time it took to reach the reaction endpoint reduced from  $8.64 \text{ hours} \pm 0.56 \text{ hours}$  (SD,  $n = 4$ , where  $n$  is the number of experiments) to  $6.52 \text{ hours} \pm 0.59 \text{ hours}$  (SD,  $n = 5$ ) ( $P < 0.001$ ). Adding  $Mg^{2+}$  to the carbonate-containing reaction solution, on the other hand, strongly inhibited the accretion of new solids (Fig. 1).

In all the accretion reactions, starting solution  $F^-$  concentrations rapidly dropped following seeding (Fig. 3) to



**Fig. 3.** Changes in free solution  $F^-$  concentrations with time for accretion reactions in which overall  $F/Ca$  was maintained at 0.01 (●) and 0.015 (○) in carbonate-free solutions, and 0.015 (▼) in solutions containing 26 mmol/liter carbonate. Error bars indicate SD of reaction points [ $n = 2-3$  (●);  $n = 3$  (○);  $n = 2-7$  (▼)].

steady solution levels that by the time the reaction endpoint was reached represented only a small percentage of the total  $F^-$  added (Table 2). Comparison of solid to overall  $F/Ca$  molar ratios (Table 3) show that most of the  $F^-$  ended up in the accreted solids. Also, since solution  $F^-$  concentrations reached steady state levels within 1 hour (Fig. 3) and overall  $F/Ca$  ratios were constant throughout the reactions, the bulk (>80%) of the new accretions had a constant  $F^-$  composition. However, even at the highest  $F/Ca$  molar ratio examined (0.07), this composition (solid  $F/Ca = 0.058$ , Table 3) was less than one third of the theoretical  $F/Ca$  molar value of 0.2 for fluorapatite. The  $Ca/PO_4$  molar ratio of the solids was unaffected by  $F^-$  but increased when carbonate was added to the system (Table 3). This latter increase could be attributed to the presence of carbonate in the accreted solids [27–30]. Although  $Mg^{2+}$  significantly slowed the accretion rate, little of this ion was taken up by the solids ( $Mg/Ca$  molar ratio =  $0.051 \pm 0.016$  (SD,  $n = 3$ ). Likewise, the effect of  $Mg^{2+}$  on  $F^-$  uptake by the solids was minimal [ $F/Ca = 0.011 \pm 0.001$  (SD,  $n = 3$ ) with  $Mg^{2+}$  versus  $0.013 \pm 0.001$  (SD,  $n = 5$ ) without  $Mg^{2+}$ ].

All solids collected at the end of the accretion experiments were apatitic in structure with no other crystalline phases detected in the X-ray diffraction patterns of the harvested solids. In experiments in which no  $F^-$ , carbonate, or  $Mg^{2+}$  was added, a threefold accretion of new solids on the apatite seed crystals increased the reciprocal of the width at one half the height (1/HW) of the 002 diffraction peak by almost twice that of the 310 peak ( $0.80^\circ 2\theta$  versus  $0.47^\circ 2\theta$ ). The percent change, however, was just the reverse; 36% and 78%, respectively, when compared with the initial seed values (Fig. 4; Table 4, bottom). These changes in 1/HW were principally the result of the accretion of new material on the seeds and not due to the maturation of the seed crystals themselves. Experiments were conducted in which the seed crystals were aged for 7 hours in the same solution milieu as used in the growth experiments, except the  $Ca^{2+}$  and  $PO_4$  concentrations were adjusted to 0.40 mmol/liter and 0.25 mmol/liter, respectively, and no titrant solutions were added. Under these conditions, there was no net change in the seed mass and the % increase was <1.5% for both 1/HW (002) and 1/HW (310).

The increase in 1/HW (002) brought about by the new accretions was not appreciably affected by  $F^-$  additions up to  $F/Ca = 0.015$ , but 1/HW (310) at this latter ratio showed a further, albeit marginal, increase (to 94.9%) (Table 4, bottom). At  $F/Ca = 0.015$ , the 310 d-spacing also decreased from 0.2270 nm to 0.2268 nm. At  $F/Ca = 0.07$ , increases in both 1/HW (002) and 1/HW (310) values were smaller than those observed in the absence of added  $F^-$  (Fig. 4).

Increases in the 1/HW values of solids harvested from accretion reactions carried out in the presence of 26 mmol/liter solution carbonate were, at 7.5% for 1/HW (002) and 13.6% for 1/HW (310) (Table 4), considerably less pronounced than those found in the absence of this anion. The presence of carbonate also shifted the 310 d-spacing to 0.2268 nm. Furthermore, the small increase in 1/HW (002) was not affected by  $F^-$  at  $F/Ca = 0.015$ . This level of  $F^-$ , however, did partially reverse the suppressive influence that carbonate had on 1/HW (310) values, with the % increase becoming greater than 2.5 times that found in the absence of  $F^-$  (Table 4). The  $F^-$  also further decreased the 310 d-spacing to 0.2265 nm. Changing the background electrolyte in the carbonate-containing experiments from  $KNO_3$  to NaCl did not alter this anisotropic  $F^-$  effect, i.e., the 1/HW (002) increase was unchanged at 9% whereas the 1/HW (310) increase doubled from 24% to 48% (Table 4).

Similarly, the anisotropy in 1/HW values observed with  $F^-$  was unaffected by the inclusion of 0.8 mmol/liter  $MgCl_2$  in the carbonate-containing solutions, although  $Mg^{2+}$  did result in a measurable increase in 1/HW (310) independent of the  $F^-$ -induced increase (Table 5). In all cases, however, the increase in 1/HW (310) values was less than one half of that observed in the absence of carbonate.

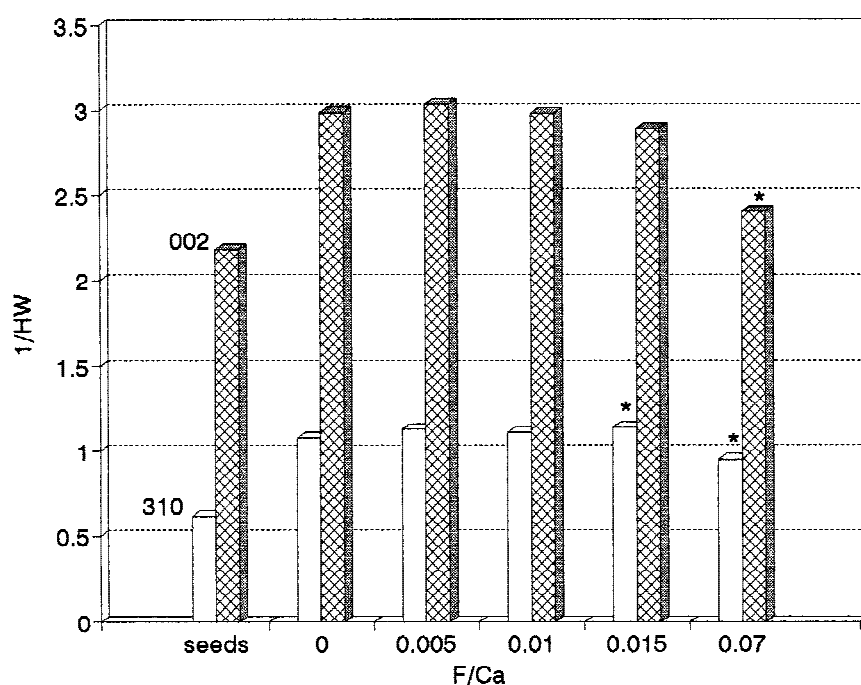
## Discussion

The solution parameters used in this study were chosen to closely simulate physiologic values. In particular, the  $Ca^{2+}$  and phosphate concentrations of 1.33 mmol/liter and 1.0 mmol/liter, respectively, fell within the range of ionic values reported for adult human serum [31]. Although IAP calculations showed that the reaction solutions under these conditions were supersaturated with respect to both OCP and HAP, the composition of the solids harvested at the end of the noncarbonated experiments were very close to that of the original apatitic seed material (Table 3). These results suggest that OCP could have formed as a transient intermediate during the course of the reactions [19] but that a non-stoichiometric apatitic phase was the principal end product, a not unexpected finding for apatite precipitated at pH 7.4 [18, 32, 33]. In the carbonate experiments, a substantial increase in the  $Ca/PO_4$  molar ratio over the seed value (Table 3), together with a contraction in the a-axis as noted by a decrease in the 310 d-spacing, suggest that carbonate was incorporated at lattice sites in the accreted apatite that otherwise would have been occupied by phosphate [27–29, 34, 35]. On the other hand,  $F^-$  incorporation did not affect the  $Ca/PO_4$  molar ratios of either noncarbonated or carbonated accretions. In the latter case, this suggests that  $F^-$  did not interfere with carbonate substitutions in the solids.

In contrast to its minimal effect on the chemical composition of the accreted solids,  $F^-$  measurably enhanced the accretion reaction in a dose-dependent manner. The rate increases were similar to those observed by Varughese and Moreno [36] and Aoba et al. [37] and were consistent with

**Table 3.** Chemical composition of filtered solids when total titrant volume equaled 3× the starting solution volume

F/Ca <sup>a</sup>	CO <sub>3</sub> <sup>b</sup>	Ca/PO <sub>4</sub> <sup>c</sup> (solids)	F/PO <sub>4</sub> <sup>c</sup> (solids)	F/Ca <sup>c</sup> (solids)
0	—	1.500 ± 0.020 (3) <sup>d</sup>		
0	+	1.690 ± 0.019 (4)		
0.005	—	1.520 ± 0.005 (2)	0.006 ± 0.001 (2)	0.004 ± 0.001 (2)
0.010	—	1.512 ± 0.001 (3)	0.012 ± 0.001 (3)	0.008 ± 0.001 (3)
0.015	—	1.507 ± 0.019 (3)	0.019 ± 0.001 (3)	0.012 ± 0.001 (3)
0.015	+	1.691 ± 0.028 (5)	0.022 ± 0.001 (5)	0.013 ± 0.001 (5)
0.070	—	1.488 ± 0.050 (3)	0.089 ± 0.002 (3)	0.058 ± 0.002 (3)
Seeds	—	1.554 ± 0.022 (3)		

<sup>a</sup> Molar F/Ca ratio of starting and titrant solutions<sup>b</sup> Reaction carried out in 26 mmol/liter NaHCO<sub>3</sub> and 5% CO<sub>3</sub>/95% N<sub>2</sub><sup>c</sup> Molar ratio<sup>d</sup> Mean ± SD; values in ( ) = number of experiments**Fig. 4.** Bar graphs showing the 1/HW values of the 310 and 002 apatite X-ray diffraction peaks for the seed material and for solids collected at the end of carbonate-free reactions in which overall F/Ca molar ratios were maintained constant at 0 to 0.07. Collected solids were 75% new accretions and 25% original seed apatite by weight. SD were  $\leq 0.04$  for the 1/HW (310) values and  $\leq 0.07$  for the 1/HW (002) values of the collected solids ( $n = 3$  except for F/Ca = 0.005 where  $n = 2$ ). Values indicated by an \* were significantly different ( $P < 0.05$ ) from corresponding control (F/Ca = 0) values.

F<sup>-</sup> increasing the thermodynamic driving force of the reaction. However, other reports [38–40] have shown that F<sup>-</sup> concentrations comparable to the steady-state levels observed in our reaction solutions reduced growth rates. Aoba [41] suggests that these apparently contradictory findings result from the coprecipitation of OCP and fluoridated apatites. The gross precipitation rate reflects a complex, highly solution-sensitive balance between the relative precipitation rates of these two phases as well as with the rate at which the OCP phase hydrolyzes to apatite. The enhanced accretion rates observed under the solution conditions used in the present study suggest that direct fluoridated apatite formation and/or accelerated OCP hydrolysis were the principal reaction pathways when F<sup>-</sup> was added to our system.

An earlier study [17] suggests that the appreciable increases in 1/HW (002) and 1/HW (310) values of solids collected from seeded reaction experiments that were carried out in the absence of added carbonate were due primarily to growth of the seed crystals. Although growth in length (002 direction) was almost twice that in width/thickness (310 direction), the percent changes in these two directions (Table 4) suggest that the seed crystals actually became somewhat bulkier as they grew. Moreover, if one assumes that the apatite crystals approximate flattened hexagonal prisms in shape and, therefore, their crystal volume ( $V_c$ ) is proportional to (length)(width/thickness)<sup>2</sup>, then the growth of the seeds in the 002 and 310 directions would fully account for the mass of new solids accreted in these

**Table 4.** Effect of F<sup>-</sup> on the reciprocals of the half-widths ( $^{\circ} 2\theta$ ) of the 002 and 310 X-ray diffraction peaks of apatite grown in 1.33 mmol/liter Ca<sup>2+</sup>, 1.0 mmol/liter tPO<sub>4</sub>, pH 7.4 solutions in the presence of 0 or 26 mmol/liter NaHCO<sub>3</sub>

	002		310	
	1/HW	Growth(%)	1/HW	Growth(%)
Seeds	2.192 ± 0.012(2) <sup>a</sup>	—	0.604 ± 0.018(2) <sup>a</sup>	—
Carbonate (KNO <sub>3</sub> )				
F/Ca = 0	2.356 ± 0.029(6) <sup>b,d</sup>	7.5	0.686 ± 0.044(6) <sup>b,d</sup>	13.6
F/Ca = 0.015	2.336 ± 0.049(7) ( <i>P</i> = 0.401)	6.6	0.822 ± 0.027(7) ( <i>P</i> = 0.0001)	36.1
Carbonate (NaCl) <sup>c</sup>				
F/Ca = 0	2.378 ± 0.013(3)	8.5	0.749 ± 0.027(3)	24.0
F/Ca = 0.015	2.386 ± 0.016(2) ( <i>P</i> = 0.578)	8.8	0.894 ± 0.050(2) ( <i>P</i> = 0.022)	48.0
No carbonate (KNO <sub>3</sub> )				
F/Ca = 0	2.990 ± 0.065(3)	36.4	1.077 ± 0.029(3)	78.3
F/Ca = 0.015	2.886 ± 0.025(3) ( <i>P</i> = 0.061)	31.7	1.177 ± 0.019(3) ( <i>P</i> = 0.007)	94.9

<sup>a,b</sup> Mean ± SD, values in ( ) = number of seed preparations<sup>a</sup> or experiments<sup>b</sup><sup>c</sup> NaCl substituted for KNO<sub>3</sub> as the background electrolyte<sup>d</sup> All experimental means were significantly different from seed values (*P* < 0.05)**Table 5.** Effect of F<sup>-</sup> on apatite seed growth in 1.33 mmol/liter Ca<sup>2+</sup>, 1.0 mmol/liter tPO<sub>4</sub>, pH 7.4 solutions in the presence of 26 mmol/liter NaHCO<sub>3</sub> and 0.8 mmol/liter MgCl<sub>2</sub><sup>a</sup>

	Percent growth <sup>b</sup>	
	002	310
no Mg <sup>2+</sup> , no F <sup>-</sup>	0.93 ± 1.23(4) <sup>c,d</sup>	10.46 ± 2.57(4) <sup>f</sup>
Mg <sup>2+</sup> , no F <sup>-</sup>	0.29 ± 0.28(3) <sup>e</sup>	18.64 ± 3.60(3) <sup>f</sup>
Mg <sup>2+</sup> , F <sup>-</sup>	3.75 ± 1.26(3) <sup>d,e</sup>	29.25 ± 3.50(3) <sup>f</sup>

<sup>a</sup> Reaction terminated when mass of new accretions became equal to the initial seed mass<sup>b</sup> Percent increase in 1/HW compared with seed value<sup>c</sup> Mean ± SD, numbers in ( ) represent number of experiments<sup>d,e,f</sup> Mean values designated with the same superscript letter are statistically different (*P* < 0.05)

reactions  $[V_c(\text{final})/V_c(\text{initial}) = 4.7 \text{ versus } 4.0 \text{ for (seeds + accretions)/(seeds)}]$ .

For F/Ca molar ratios  $\leq 0.015$ , the effect of F<sup>-</sup> on the growth of the seed crystals was marginal. The only statistically significant change (*P* < 0.05) was a slight increase in width/thickness at F/Ca = 0.015, possibly compensated by a marginal decrease in length. At F/Ca = 0.07, however, the growth in both length and width/thickness was significantly less than in the absence of added F<sup>-</sup>. This latter result suggests that the nucleation of new crystals competed with the growth of seed crystals at this higher F<sup>-</sup> level. Although the exact mechanism for generating these new crystals is not fully understood, the most likely possibility is the formation of dendritic-like outgrowths on the seed crystals that, in turn, break off into separate crystals. This secondary nucleation [42] can occur in apatite precipitation reactions when solution supersaturation is increased [17]. Since F<sup>-</sup> readily coprecipitated in our reactions, suggesting fluorapatite formation, the high residual F<sup>-</sup> concentration at F/Ca = 0.07 (20× greater than at the lower F/Ca ratios studied) (Table 2) could account for the shift to secondary nucleation in this case by contributing significantly to the supersaturated state

of the reaction milieu. The finding that F<sup>-</sup> decreased the time to reach the reaction endpoint (Fig. 2) is consistent with an increase in supersaturation [17].

Suppressed growth of the seed crystals in favor of new crystal formation was found to be even more marked in carbonate-containing reactions where mean increases in both length and width/thickness were only about 20% of that observed in the absence of this anion. This interference of carbonate with crystal growth has also been observed by others [28, 29, 35, 43, 44]. The observed increase in accretion rate with time in these reactions, as noted in Figure 1 by a positive divergence from linearity toward the end of the reaction, was also indicative of a proliferative mode of accretion. Although carbonate incorporation likely decreased the solubility of the accreted apatite [45], the initial slowing of the reaction compared with the noncarbonated control (Fig. 1) suggests that increased supersaturation may not have been a major factor in promoting the crystal proliferation in this case. On the other hand, the carbonate anions may have altered the crystal surfaces in ways that more directly favored the nucleation of readily detachable outgrowths.

The 1/HW data clearly show that F<sup>-</sup>, as well as Mg<sup>2+</sup>, partially reversed the carbonate effect and shifted the mixed pattern of proliferation and growth more toward the latter mode. Most noticeable was an increase in the mean value for width/thickness. In contrast, these ions had no stimulatory effect on growth in length. F<sup>-</sup> possibly stabilized preferentially the lateral growth faces against aberrant outgrowths thereby promoted the more orderly growth of new accretion layers on these faces by substituting for disruptive carbonate anions at OH<sup>-</sup> sites in the apatite lattice. Why this substitution did not also promote growth in length is unclear, but even in the absence of carbonate where primary seed growth predominated, the same level of F<sup>-</sup> used (F/Ca = 0.015) resulted in a propensity for increasing 1/HW (310) values at the possible expense of 1/HW (002) values (Table 4).

Although Mg<sup>2+</sup> behaved in a similar manner to F<sup>-</sup> in promoting anisotropic growth, it had to act through a dif-

ferent mechanism as this cation did not readily incorporate into the new accretions. Different mechanisms for the anisotropy was also evident from the contrasting effect these ions had on reaction kinetics. As observed by others [46–49],  $Mg^{2+}$  inhibited rather than enhanced the precipitation rate. Perhaps the slowdown in accretion, which probably resulted from  $Mg^{2+}$  interfering with  $Ca^{2+}$  ion incorporation at surface growth sites, reduced the interfacial instability that lead to outgrowths by allowing for the more orderly incorporation of other constituent ions into the lattice structure.

The size, shape, and arrangement of the apatite crystals in bone are major determinants in establishing its biomechanical properties. Alterations in these textural properties of bone apatite could contribute to the deleterious clinical features of such skeletal disorders as osteogenesis imperfecta [50]. The extracellular matrix, especially the fibrous collagenous network, appears to play an important organizational role in establishing the manner in which the crystals are arranged in this tissue as well as in placing some spatial constraints on their size and shape [51]. On the other hand, comparatively less is known about the influence of tissue fluid factors on apatite texture *in vivo*. The findings from this study suggest, however, that carbonate, and  $F^-$  when present, can be important fluid factors in this regard. In particular, our finding that carbonate was the primary reason why apatite formation in our physiologic-like aqueous solutions occurred by a proliferative mechanism suggests that this anion could be a significant factor in controlling the size of apatite crystals in skeletal tissues. Also, the finding that  $F^-$  altered mineral texture in synthetic milieus in a manner similar to that seen in bone [13, 14] and at concentrations ( $\sim 1 \mu\text{mol/liter}$ – $2 \mu\text{mol/liter}$ ) comparable to plasma levels [52] suggests that this anion selectively stimulates growth *in vivo* primarily by physicochemically interacting directly with the lateral faces of the growing bioapatite crystals and that cellular and physiologic  $F^-$  effects [52, 53] play, at most, a secondary role in this process.

**Acknowledgments.** The authors thank Drs. I. Shapiro and D. Skrtic for reviewing the manuscript and Dr. N. Eidelman for the IAP calculations.

## References

1. Roholm K (1937) Fluoride intoxication: a clinical hygienic study. H.K. Lewis, London
2. Baud CA, Bang S (1970) Fluoride and bone mineral substance. In: Vischer TL (ed) Fluoride in medicine. Hans Huber, Bern
3. Bang S (1978) Effects of fluoride on the chemical composition of inorganic bone substance. In: Courvoisier B, Donath A, Baud CA (eds) Fluoride and bone. Hans Huber, Bern
4. Eanes ED, Reddi AH (1979) The effect of fluoride on bone mineral apatite. *Metab Bone Dis Rel Res* 2:3–10
5. McCann HG, Bullock FA (1957) The effect of fluoride ingestion on the composition and solubility of mineralized tissues of the rat. *J Dent Res* 36:391–398
6. McClure FJ, McCann HG, Leone NC (1958) Excessive fluoride in water and bone chemistry. *Pub Health Rep* 73:741–746
7. Gedalia I, Menczel J, Antebi S, Zuckermann H, Pinkevski Z (1965) Calcium and phosphorus content of ash of bones and teeth of human fetuses in relation to fluoride content of drinking water. *Proc Soc Exp Biol Med* 119:694–697
8. Singer L, Armstrong WD, Zipkin I, Frazier PD (1974) Chemical composition and structure of fluorotic bone. *Clin Orthop Rel Res* 99:303–312
9. Zipkin I, McClure FJ, Lee WA (1960) Relation of the fluoride content of human bone to its chemical composition. *Arch Oral Biol* 2:190–195
10. Zipkin I, Schraer R, Schraer H, Lee WA (1963) The effect of fluoride on the citrate content of the bones of the growing rat. *Arch Oral Biol* 8:119–121
11. Gron P, McCann HG, Bernstein D (1966) Effect of fluoride on human osteoporotic bone mineral. A chemical and crystallographic study. *J Bone Joint Surg* 48-A:892–898
12. Zipkin I, Posner AS, Eanes ED (1962) The effect of fluoride on the x-ray diffraction pattern of the apatite of human bone. *Biochim Biophys Acta* 59:255–258
13. Posner AS, Eanes ED, Harper RA, Zipkin I (1963) X-ray diffraction analysis of the effect of fluoride on human bone apatite. *Arch Oral Biol* 8:549–570
14. Baud CA, Very JM, Courvoisier B (1988) Biophysical study of bone mineral in biopsies of osteoporotic patients before and after long-term treatment with fluoride. *Bone* 9:361–365
15. Eanes ED, Zipkin I, Harper RA, Posner AS (1965) Small-angle x-ray diffraction analysis of the effect of fluoride on human bone apatite. *Arch Oral Biol* 10:161–173
16. Grynblas MD (1990) Fluoride effects on bone crystals. *J Bone Miner Res* 5:S169–S175
17. Ishikawa K, Eanes ED, Tung MS (1994) The effect of supersaturation on apatite crystal formation in aqueous solutions at physiologic pH and temperature. *J Dent Res* 73:1462–1469
18. Meyer JL (1979) Hydroxyl content of solution-precipitated calcium phosphates. *Calcif Tissue Int* 27:153–160
19. Eanes ED, Meyer JL (1977) The maturation of crystalline calcium phosphates in aqueous suspensions at physiologic pH. *Calcif Tissue Res* 23:259–269
20. Ebrahimpour A, Zhang J, Nancollas GH (1991) Dual constant composition method and its application to studies of phase transformation and crystallization of mixed phases. *J Crystal Growth* 113:83–91
21. McDowell H, Gregory TM, Brown WE (1977) Solubility of  $Ca_5(PO_4)_3OH$  in the system  $Ca(OH)_2$ – $H_3PO_4$ – $H_2O$  at 5, 15, 25 and 37°C. *J Res Natl Bur Stand* 81A:273–281
22. Gregory TM, Moreno EC, Brown WE (1970) Solubility of  $CaH(PO_4) \cdot 2H_2O$  in the system  $Ca(OH)_2$ – $H_3PO_4$ – $H_2O$  at 5, 15, 25 and 37°C. *J Res Natl Bur Stand* 74A:461–475
23. Tung MS, Eidelman N, Sieck B, Brown WE (1988) Octacalcium phosphate solubility product from 4 to 37°C. *J Res Natl Bur Stand* 93:613–624
24. McCann HG (1968) The solubility of fluorapatite and its relationship to that of calcium fluoride. *Arch Oral Biol* 13:987–1001
25. Murphy J, Riley JP (1962) A modified single solution method for the determination of phosphate in natural waters. *Anal Chim Acta* 27:31–36
26. Klug HP, Alexander LE (1962) X-ray diffraction procedures. John Wiley and Sons, New York
27. LeGeros RZ (1991) Calcium phosphates in oral biology and medicine. Karger, Basel
28. Tochon-Danguy HJ, Geoffroy M, Baud CA (1980) Electron-spin resonance study of the effects of carbonate substitution in synthetic apatites and apatites from human teeth. *Arch Oral Biol* 25:357–361
29. Okazaki M, Moriwaki Y, Aoba T, Doi Y, Takahashi J, Kimura H (1982) Crystallinity changes of  $CO_3$ -apatites in solutions at physiological pH. *Caries Res* 16:308–314
30. Nelson DGA, McLean JD, Sanders JV (1983) A high-resolution electron microscope study of synthetic and biological carbonated apatites. *J Ultrastruct Res* 84:1–15
31. Kaplan A, Jack R, Opheim KE, Toivola B, Lyon AW (1995) Clinical chemistry, interpretation and techniques. Williams and Wilkins, Baltimore
32. Nancollas GH, LoRe M, Perez L, Richardson C, Zawacki SJ (1989) Mineral phases of calcium phosphate. *Anat Rec* 224:234–241
33. Nancollas GH, Zawacki SJ (1989) Calcium phosphate mineralization. *Connect Tissue Res* 21:239–244

34. LeGeros RZ (1965) Effect of carbonate on the lattice parameters of apatite. *Nature* 206:403–404
35. Nelson DGA, Featherstone JDB (1982) Preparation, analysis, and characterization of carbonated apatites. *Calcif Tissue Int* 34(suppl 2):S69–S81
36. Varughese K, Moreno EC (1981) Crystal growth of calcium apatites in dilute solutions containing fluoride. *Calcif Tissue Int* 33:431–439
37. Aoba T, Yoshioka C, Yagi T (1985) The influence of small amounts of fluoride on calcium phosphate precipitation in dilute supersaturated solutions upon hydroxyapatite seedings. *J Osaka Univ Dent Sch* 25:35–47
38. Meyer JL, Nancollas GH (1972) Effect of stannous and fluoride ions on the rate of crystal growth of hydroxyapatite. *J Dent Res* 51:1443–1450
39. Amjad Z, Nancollas GH (1979) Effect of fluoride on the growth of hydroxyapatite and human dental enamel. *Caries Res* 13:250–258
40. Eanes ED (1980) The influence of fluoride on the seeded growth of apatite from stable supersaturated solutions at pH 7.4. *J Dent Res* 59:144–150
41. Aoba T (1997) The effect of fluoride on apatite structure and growth. *Crit Rev Oral Biol Med* 8:136–153
42. Garside J (1982) Nucleation. In: Nancollas GH (ed) *Biological mineralization and demineralization*. Springer-Verlag, Berlin, pp 23–35
43. LeGeros RZ, Trautz OR, LeGeros JP, Klein E, Shirra WP (1967) Apatite crystallites: effects of carbonate on morphology. *Science* 155:1409–1411
44. Shimoda S, Aoba T, Moreno EC, Miake Y (1990) Effect of solution composition on morphological and structural features of carbonated calcium apatites. *J Dent Res* 69:1731–1740
45. Moreno EC, Aoba T (1991) Comparative solubility study of human dental enamel, dentin, and hydroxyapatite. *Calcif Tissue Int* 49:6–13
46. Tomazic B, Tomson M, Nancollas GH (1975) Growth of calcium phosphates on hydroxyapatite crystals: the effect of magnesium. *Arch Oral Biol* 20:803–808
47. Eanes ED, Rattner SL (1981) The effect of magnesium on apatite formation in seeded supersaturated solutions at pH 7.4. *J Dent Res* 60:1719–1723
48. Amjad Z, Koutsoukos PG, Nancollas GH (1984) The crystallization of hydroxyapatite and fluorapatite in the presence of magnesium ions. *J Colloid Interface Sci* 101:250–256
49. Okazaki M (1991) Crystallographic behavior of fluoridated hydroxyapatites containing  $Mg^{2+}$  and  $CO_3^{2-}$  ions. *Biomaterials* 12:831–835
50. Vetter U, Eanes ED, Kopp JB, Termine JD, Gehron Robey P (1991) Changes in apatite crystal size in bones of patients with osteogenesis imperfecta. *Calcif Tissue Int* 49:248–250
51. Glimcher MJ (1976) Composition, structure, and organization of bone and other mineralized tissues and the mechanism of calcification. In: Greep RO, Astwood EB (eds) *Handbook of physiology: endocrinology VII*. Williams and Wilkins, Baltimore, pp 25–116
52. Whitford GM (1990) The physiological and toxicological characteristics of fluoride. *J Dent Res* 69:539–549
53. Gruber HE, Baylink DJ (1991) The effects of fluoride on bone. *Clin Orthop Rel Res* 267:264–277